

UC Irvine

UC Irvine Previously Published Works

Title

Observation of $\eta' \rightarrow \pi^+\pi^-\pi^+\pi^-$ and $\eta' \rightarrow \pi^+\pi^-\pi^0\pi^0$

Permalink

<https://escholarship.org/uc/item/38w456t1>

Journal

Physical Review Letters, 112(25)

ISSN

0031-9007

Authors

Ablikim, M

Achasov, MN

Ai, XC

et al.

Publication Date

2014-06-27

DOI

10.1103/physrevlett.112.251801

Copyright Information

This work is made available under the terms of a Creative Commons Attribution License, available at <https://creativecommons.org/licenses/by/4.0/>

Peer reviewed

Observation of $\eta' \rightarrow \pi^+\pi^-\pi^+\pi^-$ and $\eta' \rightarrow \pi^+\pi^-\pi^0\pi^0$

M. Ablikim¹, M. N. Achasov^{8,a}, X. C. Ai¹, O. Albayrak⁴, M. Albrecht³, D. J. Ambrose⁴¹, F. F. An¹, Q. An⁴², J. Z. Bai¹, R. Baldini Ferroli^{19A}, Y. Ban²⁸, J. V. Bennett¹⁸, M. Bertani^{19A}, J. M. Bian⁴⁰, E. Boger^{21,b}, O. Bondarenko²², I. Boyko²¹, S. Braun³⁷, R. A. Briere⁴, H. Cai⁴⁷, X. Cai¹, O. Cakir^{36A}, A. Calcaterra^{19A}, G. F. Cao¹, S. A. Cetin^{36B}, J. F. Chang¹, G. Chelkov^{21,b}, G. Chen¹, H. S. Chen¹, J. C. Chen¹, M. L. Chen¹, S. J. Chen²⁶, X. Chen¹, X. R. Chen²³, Y. B. Chen¹, H. P. Cheng¹⁶, X. K. Chu²⁸, Y. P. Chu¹, D. Cronin-Hennessy⁴⁰, H. L. Dai¹, J. P. Dai¹, D. Dedovich²¹, Z. Y. Deng¹, A. Denig²⁰, I. Denysenko²¹, M. Destefanis^{45A,45C}, W. M. Ding³⁰, Y. Ding²⁴, C. Dong²⁷, J. Dong¹, L. Y. Dong¹, M. Y. Dong¹, S. X. Du⁴⁹, J. Z. Fan³⁵, J. Fang¹, S. S. Fang¹, Y. Fang¹, L. Fava^{45B,45C}, C. Q. Feng⁴², C. D. Fu¹, O. Fuks^{21,b}, Q. Gao¹, Y. Gao³⁵, C. Geng⁴², K. Goetzen⁹, W. X. Gong¹, W. Gradl²⁰, M. Greco^{45A,45C}, M. H. Gu¹, Y. T. Gu¹¹, Y. H. Guan¹, A. Q. Guo²⁷, L. B. Guo²⁵, T. Guo²⁵, Y. P. Guo²⁰, Y. P. Guo²⁷, Y. L. Han¹, F. A. Harris³⁹, K. L. He¹, M. He¹, Z. Y. He²⁷, T. Held³, Y. K. Heng¹, Z. L. Hou¹, C. Hu²⁵, H. M. Hu¹, J. F. Hu³⁷, T. Hu¹, G. M. Huang⁵, G. S. Huang⁴², H. P. Huang⁴⁷, J. S. Huang¹⁴, L. Huang¹, X. T. Huang³⁰, Y. Huang²⁶, T. Hussain⁴⁴, C. S. Ji⁴², Q. Ji¹, Q. P. Ji²⁷, X. B. Ji¹, X. L. Ji¹, L. L. Jiang¹, L. W. Jiang⁴⁷, X. S. Jiang¹, J. B. Jiao³⁰, Z. Jiao¹⁶, D. P. Jin¹, S. Jin¹, T. Johansson⁴⁶, N. Kalantar-Nayestanaki²², X. L. Kang¹, X. S. Kang²⁷, M. Kavatsyuk²², B. Kloss²⁰, B. Kopf³, M. Kornicer³⁹, W. Kuehn³⁷, A. Kupsc⁴⁶, W. Lai¹, J. S. Lange³⁷, M. Lara¹⁸, P. Larin¹³, M. Leyhe³, C. H. Li¹, Cheng Li⁴², Cui Li⁴², D. Li¹⁷, D. M. Li⁴⁹, F. Li¹, G. Li¹, H. B. Li¹, H. J. Li¹⁴, J. C. Li¹, K. Li¹², K. Li³⁰, Lei Li¹, P. R. Li³⁸, Q. J. Li¹, T. Li³⁰, W. D. Li¹, W. G. Li¹, X. L. Li³⁰, X. N. Li¹, X. Q. Li²⁷, Z. B. Li³⁴, H. Liang⁴², Y. F. Liang³², Y. T. Liang³⁷, D. X. Lin¹³, B. J. Liu¹, C. L. Liu⁴, C. X. Liu¹, F. H. Liu³¹, Fang Liu¹, Feng Liu⁵, H. B. Liu¹¹, H. H. Liu¹⁵, H. M. Liu¹, J. Liu¹, J. P. Liu⁴⁷, K. Liu³⁵, K. Y. Liu²⁴, P. L. Liu³⁰, Q. Liu³⁸, S. B. Liu⁴², X. Liu²³, Y. B. Liu²⁷, Z. A. Liu¹, Zhiqiang Liu¹, Zhiqing Liu²⁰, H. Loehner²², X. C. Lou^{1,c}, G. R. Lu¹⁴, H. J. Lu¹⁶, H. L. Lu¹, J. G. Lu¹, X. R. Lu³⁸, Y. Lu¹, Y. P. Lu¹, C. L. Luo²⁵, M. X. Luo⁴⁸, T. Luo³⁹, X. L. Luo¹, M. Lv¹, F. C. Ma²⁴, H. L. Ma¹, Q. M. Ma¹, S. Ma¹, T. Ma¹, X. Y. Ma¹, F. E. Maas¹³, M. Maggiora^{45A,45C}, Q. A. Malik⁴⁴, Y. J. Mao²⁸, Z. P. Mao¹, J. G. Messchendorp²², J. Min¹, T. J. Min¹, R. E. Mitchell¹⁸, X. H. Mo¹, Y. J. Mo⁵, H. Moeini²², C. Morales Morales¹³, K. Moriya¹⁸, N. Yu. Muchnoi^{8,a}, H. Muramatsu⁴⁰, Y. Nefedov²¹, I. B. Nikolaev^{8,a}, Z. Ning¹, S. Nisar⁷, X. Y. Niu¹, S. L. Olsen²⁹, Q. Ouyang¹, S. Pacetti^{19B}, M. Pelizaeus³, H. P. Peng⁴², K. Peters⁹, J. L. Ping²⁵, R. G. Ping¹, R. Poling⁴⁰, N. Q. Q⁴⁷, M. Qi²⁶, S. Qian¹, C. F. Qiao³⁸, L. Q. Qin³⁰, X. S. Qin¹, Y. Qin²⁸, Z. H. Qin¹, J. F. Qiu¹, K. H. Rashid⁴⁴, C. F. Redmer²⁰, M. Ripka²⁰, G. Rong¹, X. D. Ruan¹¹, A. Sarantsev^{21,d}, K. Schoenning⁴⁶, S. Schumann²⁰, W. Shan²⁸, M. Shao⁴², C. P. Shen², X. Y. Shen¹, H. Y. Sheng¹, M. R. Shepherd¹⁸, W. M. Song¹, X. Y. Song¹, S. Spataro^{45A,45C}, B. Spruck³⁷, G. X. Sun¹, J. F. Sun¹⁴, S. S. Sun¹, Y. J. Sun⁴², Y. Z. Sun¹, Z. J. Sun¹, Z. T. Sun⁴², C. J. Tang³², X. Tang¹, I. Tapan^{36C}, E. H. Thorndike⁴¹, D. Toth⁴⁰, M. Ullrich³⁷, I. Uman^{36B}, G. S. Varner³⁹, B. Wang²⁷, D. Wang²⁸, D. Y. Wang²⁸, K. Wang¹, L. L. Wang¹, L. S. Wang¹, M. Wang³⁰, P. Wang¹, P. L. Wang¹, Q. J. Wang¹, S. G. Wang²⁸, W. Wang¹, X. F. Wang³⁵, Y. D. Wang^{19A}, Y. F. Wang¹, Y. Q. Wang²⁰, Z. Wang¹, Z. G. Wang¹, Z. H. Wang⁴², Z. Y. Wang¹, D. H. Wei¹⁰, J. B. Wei²⁸, P. Weidenkaff²⁰, S. P. Wen¹, M. Werner³⁷, U. Wiedner³, M. Wolke⁴⁰, L. H. Wu¹, N. Wu¹, Z. Wu¹, L. G. Xia³⁵, Y. Xia¹⁷, D. Xiao¹, Z. J. Xiao²⁵, Y. G. Xie¹, Q. L. Xiu¹, G. F. Xu¹, L. Xu¹, Q. J. Xu¹², Q. N. Xu³⁸, X. P. Xu³³, Z. Xue¹, L. Yan⁴², W. B. Yan⁴², W. C. Yan⁴², Y. H. Yan¹⁷, H. X. Yang¹, L. Yang⁴⁷, Y. Yang⁵, Y. X. Yang¹⁰, H. Ye¹, M. Ye¹, M. H. Ye⁶, B. X. Yu¹, C. X. Yu²⁷, H. W. Yu²⁸, J. S. Yu²³, S. P. Yu³⁰, C. Z. Yuan¹, W. L. Yuan²⁶, Y. Yuan¹, A. A. Zafar⁴⁴, A. Zallo^{19A}, S. L. Zang²⁶, Y. Zeng¹⁷, B. X. Zhang¹, B. Y. Zhang¹, C. Zhang²⁶, C. B. Zhang¹⁷, C. C. Zhang¹, D. H. Zhang¹, H. H. Zhang³⁴, H. Y. Zhang¹, J. J. Zhang¹, J. Q. Zhang¹, J. W. Zhang¹, J. Y. Zhang¹, J. Z. Zhang¹, S. H. Zhang¹, X. J. Zhang¹, X. Y. Zhang³⁰, Y. Zhang¹, Y. H. Zhang¹, Z. H. Zhang⁵, Z. P. Zhang⁴², Z. Y. Zhang⁴⁷, G. Zhao¹, J. W. Zhao¹, Lei Zhao⁴², Ling Zhao¹, M. G. Zhao²⁷, Q. Zhao¹, Q. W. Zhao¹, S. J. Zhao⁴⁹, T. C. Zhao¹, X. H. Zhao²⁶, Y. B. Zhao¹, Z. G. Zhao⁴², A. Zhemchugov^{21,b}, B. Zheng⁴³, J. P. Zheng¹, Y. H. Zheng³⁸, B. Zhong²⁵, L. Zhou¹, Li Zhou²⁷, X. Zhou⁴⁷, X. K. Zhou³⁸, X. R. Zhou⁴², X. Y. Zhou¹, K. Zhu¹, K. J. Zhu¹, X. L. Zhu³⁵, Y. C. Zhu⁴², Y. S. Zhu¹, Z. A. Zhu¹, J. Zhuang¹, B. S. Zou¹, J. H. Zou¹

(BESIII Collaboration)

¹ Institute of High Energy Physics, Beijing 100049, People's Republic of China

² Beihang University, Beijing 100191, People's Republic of China

³ Bochum Ruhr-University, D-44780 Bochum, Germany

⁴ Carnegie Mellon University, Pittsburgh, Pennsylvania 15213, USA

⁵ Central China Normal University, Wuhan 430079, People's Republic of China

⁶ China Center of Advanced Science and Technology, Beijing 100190, People's Republic of China

⁷ COMSATS Institute of Information Technology, Lahore, Defence Road, Off Raiwind Road, 54000 Lahore

⁸ G.I. Budker Institute of Nuclear Physics SB RAS (BINP), Novosibirsk 630090, Russia

⁹ GSI Helmholtzcentre for Heavy Ion Research GmbH, D-64291 Darmstadt, Germany

¹⁰ Guangxi Normal University, Guilin 541004, People's Republic of China

¹¹ Guangxi University, Nanning 530004, People's Republic of China

¹² Hangzhou Normal University, Hangzhou 310036, People's Republic of China

¹³ Helmholtz Institute Mainz, Johann-Joachim-Becher-Weg 45, D-55099 Mainz, Germany

¹⁴ Henan Normal University, Xinxiang 453007, People's Republic of China

¹⁵ Henan University of Science and Technology, Luoyang 471003, People's Republic of China

¹⁶ Huangshan College, Huangshan 245000, People's Republic of China

- ¹⁷ *Hunan University, Changsha 410082, People's Republic of China*
¹⁸ *Indiana University, Bloomington, Indiana 47405, USA*
¹⁹ *(A)INFN Laboratori Nazionali di Frascati, I-00044, Frascati, Italy; (B)INFN and University of Perugia, I-06100, Perugia, Italy*
²⁰ *Johannes Gutenberg University of Mainz, Johann-Joachim-Becher-Weg 45, D-55099 Mainz, Germany*
²¹ *Joint Institute for Nuclear Research, 141980 Dubna, Moscow region, Russia*
²² *KVI, University of Groningen, NL-9747 AA Groningen, The Netherlands*
²³ *Lanzhou University, Lanzhou 730000, People's Republic of China*
²⁴ *Liaoning University, Shenyang 110036, People's Republic of China*
²⁵ *Nanjing Normal University, Nanjing 210023, People's Republic of China*
²⁶ *Nanjing University, Nanjing 210093, People's Republic of China*
²⁷ *Nankai University, Tianjin 300071, People's Republic of China*
²⁸ *Peking University, Beijing 100871, People's Republic of China*
²⁹ *Seoul National University, Seoul, 151-747 Korea*
³⁰ *Shandong University, Jinan 250100, People's Republic of China*
³¹ *Shanxi University, Taiyuan 030006, People's Republic of China*
³² *Sichuan University, Chengdu 610064, People's Republic of China*
³³ *Soochow University, Suzhou 215006, People's Republic of China*
³⁴ *Sun Yat-Sen University, Guangzhou 510275, People's Republic of China*
³⁵ *Tsinghua University, Beijing 100084, People's Republic of China*
³⁶ *(A)Ankara University, Dogol Caddesi, 06100 Tandogan, Ankara, Turkey; (B)Dogus University, 34722 Istanbul, Turkey; (C)Uludag University, 16059 Bursa, Turkey*
³⁷ *Universitaet Giessen, D-35392 Giessen, Germany*
³⁸ *University of Chinese Academy of Sciences, Beijing 100049, People's Republic of China*
³⁹ *University of Hawaii, Honolulu, Hawaii 96822, USA*
⁴⁰ *University of Minnesota, Minneapolis, Minnesota 55455, USA*
⁴¹ *University of Rochester, Rochester, New York 14627, USA*
⁴² *University of Science and Technology of China, Hefei 230026, People's Republic of China*
⁴³ *University of South China, Hengyang 421001, People's Republic of China*
⁴⁴ *University of the Punjab, Lahore-54590, Pakistan*
⁴⁵ *(A)University of Turin, I-10125, Turin, Italy; (B)University of Eastern Piedmont, I-15121, Alessandria, Italy; (C)INFN, I-10125, Turin, Italy*
⁴⁶ *Uppsala University, Box 516, SE-75120 Uppsala*
⁴⁷ *Wuhan University, Wuhan 430072, People's Republic of China*
⁴⁸ *Zhejiang University, Hangzhou 310027, People's Republic of China*
⁴⁹ *Zhengzhou University, Zhengzhou 450001, People's Republic of China*
- ^a *Also at the Novosibirsk State University, Novosibirsk, 630090, Russia*
^b *Also at the Moscow Institute of Physics and Technology, Moscow 141700, Russia*
^c *Also at University of Texas at Dallas, Richardson, Texas 75083, USA*
^d *Also at the PNPI, Gatchina 188300, Russia*

Using a sample of 1.3×10^9 J/ψ events collected with the BESIII detector, we report the first observation of $\eta' \rightarrow \pi^+\pi^-\pi^+\pi^-$ and $\eta' \rightarrow \pi^+\pi^-\pi^0\pi^0$. The measured branching fractions are $\mathcal{B}(\eta' \rightarrow \pi^+\pi^-\pi^+\pi^-) = (8.53 \pm 0.69(\text{stat.}) \pm 0.64(\text{syst.})) \times 10^{-5}$ and $\mathcal{B}(\eta' \rightarrow \pi^+\pi^-\pi^0\pi^0) = (1.82 \pm 0.35(\text{stat.}) \pm 0.18(\text{syst.})) \times 10^{-4}$, which are consistent with theoretical predictions based on a combination of chiral perturbation theory and vector-meson dominance.

PACS numbers: 13.25.Jx, 13.20.Gd

The η' meson is much heavier than the Goldstone bosons of broken chiral symmetry, and it has a special role in hadron physics because of its interpretation as a singlet state arising due to the axial $U(1)$ anomaly [1, 2]. Discovered in 1964 [3, 4], it remains a subject of extensive theoretical studies aiming at extensions of chiral perturbation theory [5].

New insight might be provided by the four-pion decays of η' . The strong decays $\eta' \rightarrow \pi^+\pi^-\pi^{+(0)}\pi^{-(0)}$ are not suppressed by approximate symmetries; they are expected to be mediated by chiral anomalies, since an odd number (five) of pseudoscalar particles are involved. In

particular, a contribution from a new type of anomaly, the pentagon anomaly, might show up. There should be also a significant contribution from the intermediate state with two ρ mesons. The four-pion decays have not yet been observed, and the best upper limits until now come from the CLEO collaboration: $\mathcal{B}(\eta' \rightarrow \pi^+\pi^-\pi^+\pi^-) < 2.4 \times 10^{-4}$ and $\mathcal{B}(\eta' \rightarrow \pi^+\pi^-\pi^0\pi^0) < 2.6 \times 10^{-3}$ at the 90% confidence level (C.L.) [6]. Three decades ago, a theoretical calculation using the broken- $SU_6 \times O_3$ quark model [7] yielded a branching ratio of 1.0×10^{-3} for $\mathcal{B}(\eta' \rightarrow \pi^+\pi^-\pi^{+(0)}\pi^{-(0)})$. For $\eta' \rightarrow \pi^+\pi^-\pi^+\pi^-$, this value has already been excluded by the CLEO limit. Re-

cently Guo, Kubis and Wirzba [8], using a combination of chiral perturbation theory (ChPT) and a vector-meson dominance (VMD) model, obtained the following prediction: $\mathcal{B}(\eta' \rightarrow \pi^+\pi^-\pi^+\pi^-) = (1.0 \pm 0.3) \times 10^{-4}$ and $\mathcal{B}(\eta' \rightarrow \pi^+\pi^-\pi^0\pi^0) = (2.4 \pm 0.7) \times 10^{-4}$. In this Letter, we report the first observation of $\eta' \rightarrow \pi^+\pi^-\pi^+\pi^-$ and $\eta' \rightarrow \pi^+\pi^-\pi^0\pi^0$ decays coming from $J/\psi \rightarrow \gamma\eta'$ radiative decay events using a sample of 1.3×10^9 J/ψ events (2.25×10^8 events [9] in 2009 and 1.09×10^9 in 2012) [10] taken at the center of mass energy of 3.097 GeV with the BESIII detector.

The BESIII detector is a magnetic spectrometer [11] located at the Beijing Electron Positron Collider (BEPCII), which is a double-ring e^+e^- collider with a design peak luminosity of $10^{33} \text{ cm}^{-2}\text{s}^{-1}$ at the center of mass energy of 3.773 GeV. The cylindrical core of the BESIII detector consists of a helium-based main drift chamber (MDC), a plastic scintillator time-of-flight system (TOF), and a CsI(Tl) electromagnetic calorimeter (EMC), which are all enclosed in a superconducting solenoidal magnet providing a 1.0 T (0.9 T in 2012) magnetic field. The solenoid is supported by an octagonal flux-return yoke with resistive plate counter muon identifier modules interleaved with steel. The acceptance of charged particles and photons is 93% over 4π solid angle. The charged-particle momentum resolution at $1 \text{ GeV}/c^2$ is 0.5%, and the dE/dx resolution is 6%. The EMC measures photon energies with a resolution of 2.5% (5%) at 1 GeV in the barrel (endcaps). The time resolution of TOF is 80 ps in the barrel and 110 ps in the end caps.

Monte Carlo (MC) simulations are used to estimate backgrounds and determine detection efficiencies. Simulated events are processed using GEANT4 [12, 13], where measured detector resolutions are incorporated.

For $J/\psi \rightarrow \gamma\eta'$ with $\eta' \rightarrow \pi^+\pi^-\pi^+\pi^-$, candidate events are required to have four charged tracks and at least one photon. Each charged track, reconstructed using hits in the MDC, is required to be in the polar range $|\cos\theta| < 0.93$ and pass within 10 cm in the beam direction and within 1 cm in the radial direction, with respect to the interaction point. For each charged track, the TOF and dE/dx information are combined to form particle identification confidence levels for the π , K , and p hypotheses, and the particle type with the highest C.L. is assigned to each track. At least two oppositely charged tracks are required to be identified as pions. Photon candidates, reconstructed by clustering EMC crystal energies, must have at least 25 MeV of energy for barrel showers ($|\cos\theta| < 0.8$), or 50 MeV for endcap showers ($0.86 < |\cos\theta| < 0.92$). To exclude showers from charged particles, the angle between the nearest charged track and the shower must be greater than 10° . Further, EMC cluster timing requirements are used to suppress electronic noise and energy deposits unrelated to the event.

Next a four-constraint (4C) kinematic fit imposing energy-momentum conservation is performed under the

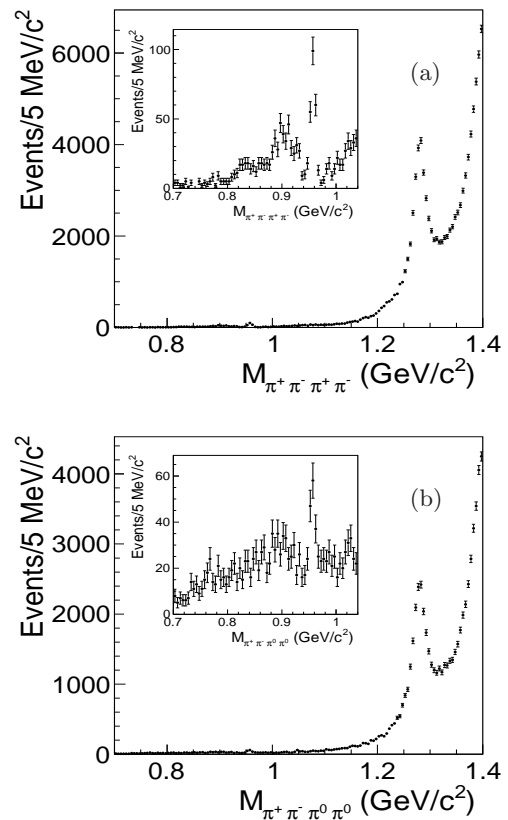


Figure 1: The invariant mass distributions of (a) $\pi^+\pi^-\pi^+\pi^-$ and (b) $\pi^+\pi^-\pi^0\pi^0$ after the final selection. The inserts are for the mass spectra around the η' mass region.

$\gamma\pi^+\pi^-\pi^+\pi^-$ hypothesis, and a loose requirement of $\chi_{4C}^2 < 35$ is imposed. If there is more than one photon candidate in an event, the combination with the smallest χ_{4C}^2 is retained, and its χ_{4C}^2 is required to be less than that for the $\gamma\pi^+\pi^-\pi^+\pi^-$ hypothesis. The $\pi^+\pi^-\pi^+\pi^-$ invariant mass spectrum for the selected events is shown in Fig. 1(a), where an η' peak is clearly observed in the inset plot.

To ensure that the η' peak is not from background, a study was performed with a MC sample of 1 billion J/ψ events generated with the Lund model [14]. The results indicate that the enhancement below the η' peak in Fig. 1(a) is from the background channel $\eta' \rightarrow \pi^+\pi^-\eta$ with $\eta \rightarrow \gamma\pi^+\pi^-$, while the background in the mass region above $1 \text{ GeV}/c^2$ is mainly from $\eta' \rightarrow \pi^+\pi^-e^+e^-$. Other background channels are $J/\psi \rightarrow \gamma f_2(1270), f_2(1270) \rightarrow \pi^+\pi^-\pi^+\pi^-$ and non-resonant $J/\psi \rightarrow \gamma\pi^+\pi^-\pi^+\pi^-$. However, none of these background sources produces a peak in the $\pi^+\pi^-\pi^+\pi^-$ invariant mass spectrum near the η' mass.

For $J/\psi \rightarrow \gamma\eta'$ with $\eta' \rightarrow \pi^+\pi^-\pi^0\pi^0$, candidate events must have two charged tracks with zero net charge, that are identified as pions, and at least five photons. One-constraint (1C) kinematic fits are performed on the π^0

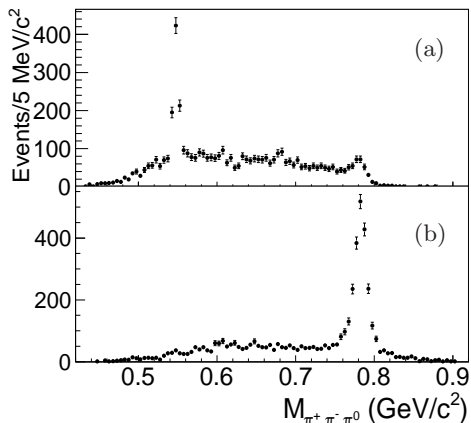


Figure 2: The $\pi^+\pi^-\pi^0$ invariant mass distributions for the combinations closest to (a) m_η and (b) m_ω .

candidates reconstructed from photon pairs with the invariant mass of the two photons being constrained to the π^0 mass, and $\chi^2_{1C}(\gamma\gamma) < 50$ is required. Then a six-constraint (6C) kinematic fit (two π^0 masses are also constrained) is performed under the hypothesis of $J/\psi \rightarrow \gamma\pi^+\pi^-\pi^0\pi^0$. For events with more than two π^0 candidates, the combination with the smallest χ^2_{6C} is retained. A rather loose criterion of $\chi^2 < 35$ is required to exclude events with a kinematics incompatible with the signal hypothesis. To reject background from events with six photons in the final state, χ^2_{6C} is required to be less than that for the $\gamma\gamma\pi^+\pi^-\pi^0\pi^0$ hypothesis. After this selection, Figs. 2(a) and (b) show the invariant mass of the $\pi^+\pi^-\pi^0$ combination closest to the nominal η or ω mass (denoted as m_η and m_ω), respectively. Significant η and ω peaks are seen. These backgrounds are suppressed by rejecting events with $|M_{\pi^+\pi^-\pi^0} - m_\eta| < 0.02 \text{ GeV}/c^2$ or $|M_{\pi^+\pi^-\pi^0} - m_\omega| < 0.02 \text{ GeV}/c^2$.

After the above selection, Fig. 1(b) shows the $\pi^+\pi^-\pi^0\pi^0$ invariant mass distribution, where an η' peak is very clear. With the MC sample of 1 billion J/ψ events, the same study for $\eta' \rightarrow \pi^+\pi^-\pi^0\pi^0$ was also performed to investigate possible background events, and the main backgrounds were found to come from: (1) $\eta' \rightarrow \pi^+\pi^-\eta$, $\eta \rightarrow \pi^0\pi^0\pi^0$, (2) $\eta' \rightarrow \pi^0\pi^0\eta$, $\eta \rightarrow \gamma\pi^+\pi^-$, (3) $\eta' \rightarrow \gamma\omega$, $\omega \rightarrow \pi^+\pi^-\pi^0$, and (4) $J/\psi \rightarrow \gamma f_2(1270)$, $f_2(1270) \rightarrow \pi^+\pi^-\pi^0\pi^0$ and (5) non-resonant $J/\psi \rightarrow \gamma\pi^+\pi^-\pi^0\pi^0$. None of these possible background channels contribute to the η' peak.

The signal yields are obtained from extended unbinned maximum likelihood fits to the $\pi^+\pi^-\pi^{+(0)}\pi^{-(0)}$ invariant mass distributions. The total probability density function (PDF) consists of a signal and various background contributions. The signal component is modeled as the MC simulated signal shape convoluted with a Gaussian function to account for the difference in the mass reso-

lution observed between data and MC simulation. For this analysis, MC simulation indicates that the mass resolution has almost no change for the two data sets taken in 2009 and 2012, respectively. The background components considered are subdivided into three classes: (i) the shapes of those background events that contribute to a structure in $M_{\pi^+\pi^-\pi^+\pi^-}$ [e.g., $\eta' \rightarrow \pi^+\pi^-\eta$ with $\eta \rightarrow \gamma\pi^+\pi^-$ and $\eta' \rightarrow \pi^+\pi^-e^+e^-$] or $M_{\pi^+\pi^-\pi^0\pi^0}$ [e.g., $\eta' \rightarrow \pi^+\pi^-\eta$ with $\eta \rightarrow \pi^0\pi^0\pi^0$ and $\eta' \rightarrow \pi^0\pi^0\eta$ with $\eta \rightarrow \gamma\pi^+\pi^-$, as well as $\eta' \rightarrow \gamma\omega$ with $\omega \rightarrow \pi^+\pi^-\pi^0$] are taken from the dedicated MC simulations; (ii) the tail of the resonance $f_2(1270)$ from $J/\psi \rightarrow \gamma f_2(1270)$ is parameterized with a Breit-Wigner function convoluted with a Gaussian for the mass resolution from the simulation; (iii) $J/\psi \rightarrow \gamma\pi^+\pi^-\pi^+\pi^-$ ($J/\psi \rightarrow \gamma\pi^+\pi^-\pi^0\pi^0$) phase space is also described with the MC simulation shape. In the fit to data, the mass and width of $f_2(1270)$ are fixed to the values in the PDG [15], while the magnitudes of different components are left free in the fit to account for the uncertainties of the branching fractions of $J/\psi \rightarrow \gamma\eta'$ and other intermediate decays (e.g., $\eta' \rightarrow \pi^+\pi^-\eta$, $\eta' \rightarrow \pi^0\pi^0\eta$, and $\eta \rightarrow \gamma\pi^+\pi^-$).

The projections of the fit to $M_{\pi^+\pi^-\pi^{+(0)}\pi^{-(0)}}$ in the η' mass region are shown in Figs. 3(a) and (b), where the shape of the sum of signal and background shapes is in good agreement with data. We obtain 199 ± 16 $\eta' \rightarrow \pi^+\pi^-\pi^+\pi^-$ events with a statistical significance of 18σ and 84 ± 16 $\eta' \rightarrow \pi^+\pi^-\pi^0\pi^0$ events with a statistical significance of 5σ . The statistical significance is determined by the change of the log-likelihood value and the number of degree of freedom in the fit with and without the η' signal.

In order to compute the branching fractions, the signal efficiencies for the selection criteria described above are estimated with the MC simulation. To ensure a good description of data, in addition to the phase space events, we also produced a signal MC sample in which the signal simulation is modeled as the decay amplitudes in Ref. [8] based on the ChPT and VMD model. For $\eta' \rightarrow \pi^+\pi^-\pi^+\pi^-$, we divide each of $M_{\pi^+\pi^-}$ combination into 38 bins in the region of $[0.28, 0.66] \text{ GeV}/c^2$. With the same procedure as described above, the number of the η' events in each bin can be obtained by fitting the $\pi^+\pi^-\pi^+\pi^-$ mass spectrum in this bin, and then the background-subtracted $M_{\pi^+\pi^-}$ is obtained as shown in Fig. 4 (four entries per event), where the errors are statistical only. The comparison of $M_{\pi^+\pi^-}$ between data and two different models displayed in Fig. 4 indicates that the ChPT and VMD model could provide a more reasonable description of data than the phase space events. Therefore the simulation events generated with the ChPT and VMD model are applied to determine the detection efficiency for $\eta' \rightarrow \pi^+\pi^-\pi^{+(0)}\pi^{-(0)}$ decays. Table I lists all the information used for the branching fraction measurements.

Sources of systematic errors and their corresponding

Table I: Signal yields, detection efficiencies and the product branching fractions of $J/\psi \rightarrow \gamma\eta'$, $\eta' \rightarrow \pi^+\pi^-\pi^+\pi^-$. The first errors are statistical and the second systematic.

Mode	Yield	ε (%)	Branching fraction
$\eta' \rightarrow \pi^+\pi^-\pi^+\pi^-$	199 ± 16	34.5	$(4.40 \pm 0.35 \pm 0.30) \times 10^{-7}$
$\eta' \rightarrow \pi^+\pi^-\pi^0\pi^0$	84 ± 16	7.0	$(9.38 \pm 1.79 \pm 0.89) \times 10^{-7}$

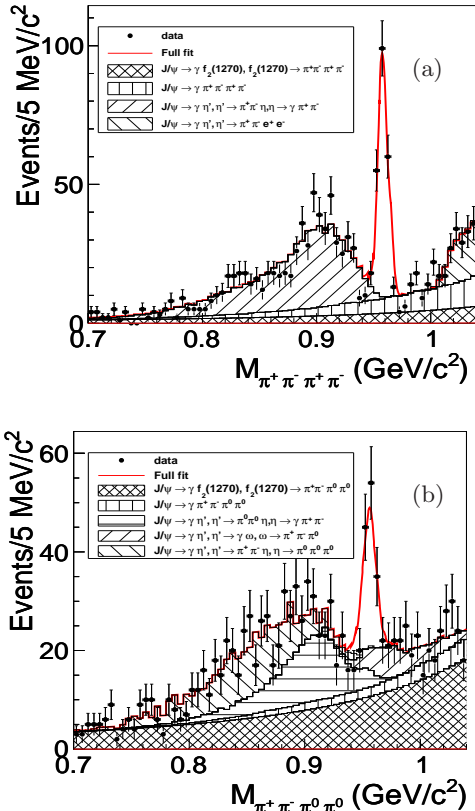


Figure 3: Results of the fits to (a) $M_{\pi^+\pi^-\pi^+\pi^-}$ and (b) $M_{\pi^+\pi^-\pi^0\pi^0}$, where the background contributions are displayed as the hatched histograms.

contributions to the measurement of the branching fractions are summarized in Table II. The uncertainties in MDC tracking and photon detection have been studied with the high purity control sample of $J/\psi \rightarrow \rho\pi$ for two data sets. The differences in the detection efficiencies between data and MC simulation are less than 1% per charged track and 1% per photon, which are taken as the systematic errors. Similarly, to estimate the error related to the pion identification, the pion identification efficiency has been studied using a clean sample of $J/\psi \rightarrow \rho\pi$, and the data is found to be in agreement with MC simulation within 1%. For $\eta' \rightarrow \pi^+\pi^-\pi^+\pi^-$, at least one π^+ and one π^- are required to be identified, and the error from this source is calculated to be 0.6%, while 2% is as-

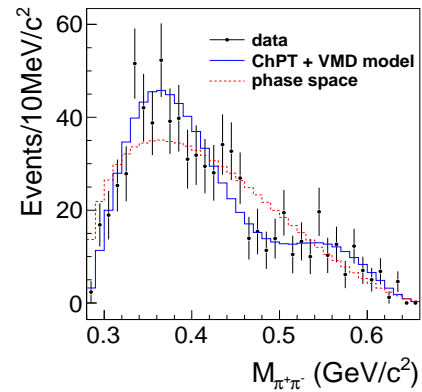


Figure 4: The comparison of $M_{\pi^+\pi^-}$ (four entries per event) between data and two different models, where the dots with error bars are for the background-subtracted data, the solid line is for the ChPT and VMD model, and the dashed line is for the phase space.

signed for $\eta' \rightarrow \pi^+\pi^-\pi^0\pi^0$ because both charged tracks are required to be identified as pions. The uncertainty arising from the ω (η) veto is estimated by varying the requirements from $|M_{\pi^+\pi^-\pi^0} - m_\omega/m_\omega| > 0.02 \text{ GeV}/c^2$ to $|M_{\pi^+\pi^-\pi^0} - m_\eta/m_\omega| > 0.018 \text{ GeV}/c^2$ in the event selection.

The uncertainty associated with the kinematic fit comes from the inconsistency between data and MC simulation of the track parameters and the error matrices. In this analysis the uncertainties arising from the kinematic fit are estimated by using $J/\psi \rightarrow \phi\eta$ events with $\phi \rightarrow K^+K^-$ and $\eta \rightarrow \pi^+\pi^-\pi^0$, which have a topology similar to the decay channels of interest. A sample is selected without a kinematic fit. The event selection for charged tracks and photons are the same as the two decays studied in this analysis. Each charged track is identified as a kaon or a pion. Then a 4C kinematic fit is performed for the candidates of $J/\psi \rightarrow \phi\eta$, $\eta \rightarrow \pi^+\pi^-\pi^0$; and a 7C kinematic fit for $J/\psi \rightarrow \phi\eta$, $\eta \rightarrow \pi^0\pi^0\pi^0$ by constraining the $\gamma\gamma$ invariant mass to be the π^0 mass. The efficiencies for $\chi^2 < 35$ are obtained by comparing the number of signal events with and without the 4C (7C) kinematic fit performed for data and MC simulation separately. The data-MC differences shown in Table II are taken as the systematic errors from this source.

Background events whose distributions peak either below (e.g., $\eta' \rightarrow \pi^+\pi^-\eta$) or just above the η' peak (e.g., $\eta' \rightarrow \gamma\omega$) may alter the signal yield. We performed an alternative fit by fixing these contributions according to the branching fractions of $J/\psi \rightarrow \gamma\eta'$ and the cascade decays and found the impact on the signal yield is small. The uncertainty associated with the smooth background functions, including the phase space shape and the tail of $f_2(1270)$, is evaluated by replacing them with a second

order polynomial, and the uncertainties of 2.1% and 3.5% are due to the yield difference with respect to the nominal fit. The uncertainties due to the fit range are considered by varying the fit ranges, and the difference of the results are 2.1% and 3.8%. The uncertainties due to the MC model are estimated with MC samples in which the signal simulation is modeled according to the decay amplitudes in Ref. [8] and a phase space distribution, and the differences are 1.4% and 4.5%, respectively.

The branching fractions for $J/\psi \rightarrow \gamma\eta'$ and $\pi^0 \rightarrow \gamma\gamma$ decays are taken from the world average values [15], and the uncertainties on these branching fractions are taken as the associated systematic uncertainty in our measurements.

All the above contributions and the uncertainty from the number of J/ψ events [10] are summarized in Table II, where the total systematic uncertainty is given by the quadratic sum of the individual errors, assuming all sources to be independent.

Table II: Summary of the systematic uncertainties in the branching fractions (in %). In the calculation of the product branching fractions of $J/\psi \rightarrow \gamma\eta', \eta' \rightarrow \pi^+\pi^-\pi^+\pi^-$, the uncertainty of $\mathcal{B}(J/\psi \rightarrow \gamma\eta')$ is not included.

Sources	$\eta' \rightarrow \pi^+\pi^-\pi^+\pi^-$	$\eta' \rightarrow \pi^+\pi^-\pi^0\pi^0$
MDC tracking	4.0	2.0
Photon detection	1.0	5.0
Particle identification	0.6	2.0
η (ω) veto	-	2.1
4C/6C kinematic fit	4.4	2.1
Continuous BG shape	2.1	3.5
Fit range	2.1	3.8
MC model	1.4	4.5
$\mathcal{B}(J/\psi \rightarrow \gamma\eta')$	2.9	2.9
$\mathcal{B}(\pi^0 \rightarrow \gamma\gamma)$	-	0.1
Number of J/ψ events	0.8	0.8
Total	7.5	9.9

In summary, based on a sample of 1.3 billion J/ψ events taken with the BESIII detector, we observe the decay modes $\eta' \rightarrow \pi^+\pi^-\pi^+\pi^-$ and $\eta' \rightarrow \pi^+\pi^-\pi^0\pi^0$ with a statistical significance of 18σ and 5σ , respectively, and measure their product branching fractions: $\mathcal{B}(J/\psi \rightarrow \gamma\eta') \cdot \mathcal{B}(\eta' \rightarrow \pi^+\pi^-\pi^+\pi^-) = (4.40 \pm 0.35(\text{stat.}) \pm 0.30(\text{syst.})) \times 10^{-7}$ and $\mathcal{B}(J/\psi \rightarrow \gamma\eta') \cdot \mathcal{B}(\eta' \rightarrow \pi^+\pi^-\pi^0\pi^0) = (9.38 \pm 1.79(\text{stat.}) \pm 0.89(\text{syst.})) \times 10^{-7}$. Using the PDG world average value of $\mathcal{B}(J/\psi \rightarrow \gamma\eta')$ [15], the branching fractions of $\eta' \rightarrow \pi^+\pi^-\pi^+\pi^-$ and $\eta' \rightarrow \pi^+\pi^-\pi^0\pi^0$ are determined to be $\mathcal{B}(\eta' \rightarrow \pi^+\pi^-\pi^+\pi^-) = (8.53 \pm 0.69(\text{stat.}) \pm 0.64(\text{syst.})) \times 10^{-5}$ and $\mathcal{B}(\eta' \rightarrow \pi^+\pi^-\pi^0\pi^0) = (1.82 \pm 0.35(\text{stat.}) \pm 0.18(\text{syst.})) \times 10^{-4}$, which are consistent with the theoretical predictions based on a combination of chiral perturbation theory and vector-meson dominance, but not with the broken-SU₆×O₃ quark model [7].

The BESIII collaboration thanks the staff of BEPCII and the computing center for their strong support. This work is supported in part by the Ministry of Science and Technology of China under Contract No. 2009CB825200; Joint Funds of the National Natural Science Foundation of China under Contracts Nos. 11079008, 11179007, U1232101, U1232107, U1332201; National Natural Science Foundation of China (NSFC) under Contracts Nos. 10625524, 10821063, 10825524, 10835001, 10935007, 11125525, 11235011, 11175189; the Chinese Academy of Sciences (CAS) Large-Scale Scientific Facility Program; CAS under Contracts Nos. KJCX2-YW-N29, KJCX2-YW-N45; 100 Talents Program of CAS; German Research Foundation DFG under Contract No. Collaborative Research Center CRC-1044; Istituto Nazionale di Fisica Nucleare, Italy; Ministry of Development of Turkey under Contract No. DPT2006K-120470; U. S. Department of Energy under Contracts Nos. DE-FG02-04ER41291, DE-FG02-05ER41374, DE-FG02-94ER40823, DESC0010118; U.S. National Science Foundation; University of Groningen (RuG) and the Helmholtzzentrum fuer Schwerionenforschung GmbH (GSI), Darmstadt; WCU Program of National Research Foundation of Korea under Contract No. R32-2008-000-10155-0.

- [1] S. Weinberg, Phys. Rev. D **11**, 3583 (1975).
- [2] G. 't Hooft, Phys. Rev. D **14** (1976) 3432 [Erratum-ibid. D **18** (1978) 2199].
- [3] G. R. Kalbfleisch *et al.*, Phys. Rev. Lett. **12**, 527 (1964).
- [4] M. Goldberg *et al.*, Phys. Rev. Lett. **12**, 546 (1964).
- [5] J. Gasser, H. Leutwyler, Nucl. Phys. B **250**, 465 (1985).
- [6] P. Naik *et al.* [CLEO Collaboration], Phys. Rev. Lett. **102**, 061801 (2009).
- [7] D. Parashar, Phys. Rev. D **19**, 268 (1979).
- [8] Feng-Kun Guo, Bastian Kubis and Andreas Wirzba, Phys. Rev. D **85**, 014014 (2012).
- [9] M. Ablikim *et al.* [BESIII Collaboration], Chin. Phys. C **36**, 915 (2012).
- [10] With the same approach as for J/ψ events taken in 2009 (see Ref. [9] for more details), the preliminary number of J/ψ events taken in 2009 and 2012 is determined to be 1310.6×10^6 with an uncertainty of 0.8%.
- [11] M. Ablikim *et al.* [BESIII Collaboration], Nucl. Instrum. Methods Phys. Res. A **614**, 345 (2010).
- [12] S. Agostinelli *et al.* [GEANT4 Collaboration], Nucl. Instrum. Methods Phys. Res. A **506**, 250 (2003).
- [13] J. Allison *et al.*, IEEE Trans. Nucl. Sci. **53**, 270 (2006).
- [14] J. C. Chen, G. S. Huang, X. R. Qi, D. H. Zhang and Y. S. Zhu, Phys. Rev. D **62**, 034003 (2000).
- [15] J. Beringer *et al.* [Particle Data Group], Phys. Rev. D **86**, 010001 (2012).
- [16] M. Ablikim *et al.* [BESIII Collaboration], Phys. Rev. D **81**, 052005 (2010).